ELSEVIER

Chemical Physics 237 (1998) 123–138

Chemical Physics

Vibrationally state-selective laser pulse control of electronic branching in OH $(X^2\Pi/A^2\Sigma^+)$ photoassociation

M.V. Korolkov [1], B. Schmidt

Institut für Physikalische und Theoretische Chemie, Freie Universität Berlin, Takustrasse 3, 14195 Berlin, Germany

Received 4 May 1998

Abstract

The quantum dynamics of photoassociative collisions $O(^3P) + H(^2S)$ controlled by picosecond laser pulses is explored in the ground $(X^2\Pi)$ and excited $(A^2\Sigma^+)$ electronic states. Coupled Schrödinger equations are solved for representative wavepackets using ab initio data for potentials and (transition) dipole moments. The effect of laser induced electronic transitions as well as the branching between products in the two electronic states is investigated. It is shown that by optimal choice of the laser pulse parameters the ground state process can be achieved with high efficiency (> 80%) and a vibrational state selectivity very close to 100%. For the excited state, similar results can be obtained by a two-pulse ''dump-pump'' strategy. The electronic branching ratio can be controlled by the frequency and the polarization of the laser pulses or the scattering energy of the collision pair.

1. Introduction

In recent years, the ultrafast laser-spectroscopic investigation of elementary chemical reactions has made enormous progress and has emerged into the new field of femtochemistry [1–4]. While there is an appreciable amount of studies on unimolecular reactions, e.g. the breaking of molecular bonds in a photodissociation process, the study of bimolecular reactions is still at its infancy. One of the simplest binary reactions is the process of bond formation in the collision of two atoms or radicals. An important possibility to form a stable molecule from an isolated collision pair is by radiative mechanisms. Apart from spontaneous emission of light which usually is much slower than the timescale of collision events, this can be achieved by photoassociation. At the same time, the stimulated nature of these processes provides a means to analyze and to control the bond formation in real time by use of ultrashort laser pulses.

Until now, most of the studies of photoassociation reactions are concerned with the excitation of free collision pairs in the electronic ground state to bound vibrational levels of an excited electronic state, see e.g. the work on alkali atoms [5–16], rare gas halides and hydrides [17–21] and on certain metals in the second column of the periodic table [22–25].

In more recent publications, first experimental studies of photoassociation by pump-probe techniques have been reported [26,27]. At the same time, first theoretical studies investigate the quantum dynamics of these processes [28–33]. In another series of papers, an alternative approach to the formation of heteronuclear molecules by photoassociation is pre-

[1] Permanent address: B.I. Stepanov Institute of Physics, National Academy of Sciences of Belarus, Skaryna ave. 70, 220602 Minsk, Republic of Belarus.

0301-0104/98/$ - see front matter
PII: S0301-0104(98)00219-5

sented. It is suggested to employ stimulated emission of light to form bound molecules in the electronic ground state [34–37]. These studies demonstrate that ground state photoassociation can be made very efficient by simultaneous optimization of laser pulses and wavepacket parameters. Furthermore, very high (close to 100%) selectivity with respect to the (ro-)vibrational state of the molecular product can be achieved.

In the present work we want to focus on the quantum dynamics of photoassociation taking into account both the ground and excited electronic state. As in our previous work on ground state photoassociation, we choose the formation of the hydroxyl (OH) molecule as an example [34–36]. Here we improve our model by using highly accurate ab initio data for both potential energy and dipole moment functions. For a model consisting of the ground ($X^2\Pi$) and the lowest bound excited state ($A^2\Sigma^+$) [38], the two pathways that can lead to formation of stable molecules are the photoassociation into the ground state by stimulated emission of light

$$O(^3P) + H(^2S) \xrightarrow{\hbar\omega} OH\left(X^2\Pi, v_g\right), \tag{1}$$

and the photoassociation in the excited electronic state by absorption of light

$$O(^3P) + H(^2S) \xrightarrow{\hbar\omega} OH\left(A^2\Sigma^+, v_e\right), \tag{2}$$

where we take into account the possibility of re-dissociation with one of the collision partners (here O) being electronically excited

$$O(^3P) + H(^2S) \xrightarrow{\hbar\omega} O(^1D) + H(^2S). \tag{3}$$

In particular, we are concerned with the following questions: (i) How efficient are the ground and excited state photoassociation processes? (ii) How can the branching be controlled? (iii) How selective are these processes with respect to the vibrational level of the molecular product? (iv) Finally, how are the results for one of the processes changed by the presence of the other process? The following section will give all the details on our model and on the numerical solution of the dynamical equations. We present our results in Section 3. Finally, our conclusions are presented in Section 4.

2. Model

In the present study, we consider photoassociative collisions in a one-dimensional (rotationless) model. The dynamics of the collision pair is treated in a quantum-mechanical wavepacket picture. The initial state of the collision pair in the electronic ground state $O(^3P) + H(^2S)$ is chosen similar to our previous studies [34,35]. We use a localized Gaussian wavepacket in the internuclear distance coordinate r

$$\psi_g(r, t=0) = \left(\frac{2}{\pi a^2}\right)^{1/4} \exp\left[iK_0 r - \left(\frac{r-r_0}{a}\right)^2\right], \tag{4}$$

where the two atoms are assumed to be initially at an average distance of $\langle r\rangle = r_0$ well outside the interaction region. The initial momentum $\langle k\rangle = K_0 < 0$ of the incident wavepacket corresponds to a relative collision energy of

$$E_0 = \frac{\hbar^2}{2m}\left(K_0^2 + 1/a^2\right), \tag{5}$$

with a relative mass of $m = 0.9482$ u for the $^{16}O + {}^1H$ collision pair.

As the atoms are approaching each other, they start to interact through the potential energy. Here we consider only the two lowest bound electronic states $V_g(X^2\Pi)$ and $V_e(A^2\Sigma^+)$ of the OH molecule. To obtain the potential energy curves we fit extended Rydberg functions [38] (see Fig. 1(a) and Ref. [39]) to the high quality ab initio data adapted from Ref. [40].

In order to describe the coupling of the wavepacket dynamics in the two electronic states to external fields, we have to include dipole moment functions in our model. Permanent dipole moment functions $\mu_g(r)$ and $\mu_e(r)$ for the ground and excited electronic state, respectively, are taken from ab initio data [41,42]. The transition dipole moment function $\mu_{g,e}(r)$ coupling the $X^2\Pi$ and the $A^2\Sigma^+$ states is also adapted from the literature [43,40] (see Fig. 1(b)). Note that $\mu_g(r)$ and $\mu_e(r)$ are parallel to the molecular axis while $\mu_{g,e}(r)$ is perpendicular. In the framework of the present rotationless model, we assume the molecule to be aligned along the x axis,

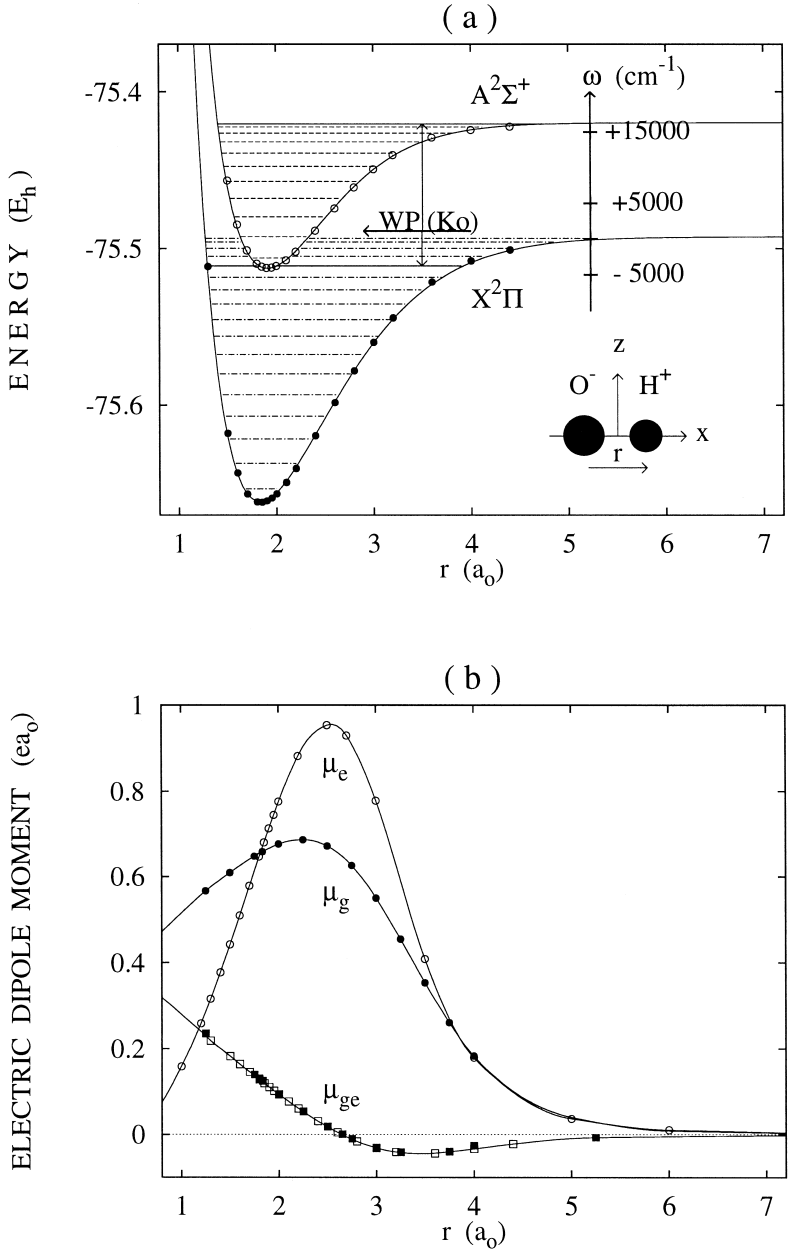

Fig. 1. (a) Ab initio data for the potential energy curves of the two lowest bound electronic states $V_g(X^2\Pi)$ and $V_e(A^2\Sigma^+)$ of the OH molecule [40]. The solid curves show a fit of the data to extended Rydberg functions, see Ref. [38]. The horizontal arrow indicates the incoming wavepacket with momentum K_0, see Eq. (4). The vertical arrows schematically represent photoassociative transitions down to the $v_g = 12$ and up to the $v_e = 10$ vibrational level. A frequency scale in cm^{-1} for these transitions is given, too. The insert indicates the orientation of the permanent dipole moments μ_g and μ_e (along x) and of the transition dipole moment $\mu_{g,e}$ (along z). (b) Ab initio data for the permanent dipole functions of ground state μ_g (solid circles [41]) and excited state μ_e (open circles [42]), and for the transition dipole moment $\mu_{g,e}$ (solid squares [56] and open squares [40]).

see insert of Fig. 1(a). We employ the semiclassical dipole approximation [44]. Hence, the time evolution of the collision pair is given by two coupled time-dependent Schrödinger equations for the wavefunctions $\psi_g(r,t)$ and $\psi_e(r,t)$ corresponding to the relative nuclear motion in the ground and excited electronic state

$$i\hbar\frac{\partial}{\partial t}\psi_g(r,t) = \left[\hat{T} + V_g(r) - \mu_g(r)\mathscr{E}_x(t)\right]\psi_g(r,t) - \mu_{g,e}(r)\mathscr{E}_z(t)\psi_e(r,t),$$
$$i\hbar\frac{\partial}{\partial t}\psi_e(r,t) = \left[\hat{T} + V_e(r) - \mu_e(r)\mathscr{E}_x(t)\right]\psi_e(r,t) - \mu_{g,e}(r)\mathscr{E}_z(t)\psi_g(r,t), \quad (6)$$

where $\hat{T}$ stands for the kinetic energy operator and where $\mathscr{E}_x(t)$ and $\mathscr{E}_z(t)$ are the components of the electric field parallel and perpendicular to the molecular axis, respectively. Laser pulses are assumed to have a $\sin^2$-shaped envelope of the electric field

$$\mathscr{E}(t) = \mathscr{E}_0 \sin^2\left(\frac{\pi(t-\delta t)}{\tau}\right)\cos\left[\omega(t-\delta t)\right], \quad \delta t \le t \le \tau + \delta t, \quad (7)$$

with amplitude $\mathscr{E}_0$, carrier frequency ω, pulse duration τ, and time delay δt.

The coupled equations (6) are solved numerically by means of a grid discretization in coordinate space [45] allowing the use of efficient fast Fourier transforms (FFT) for the evaluation of $\hat{T}$. The wave functions $\psi_g(r,t)$ and $\psi_e(r,t)$ are represented on an equidistant grid. The number of points varies from $N = 1024$ to $N = 8192$ with a distance of $\Delta r = 0.05$ a_0 (atomic units: 1 $a_0 = 5.29177 \times 10^{-11}$ m). A ''gobbler'' function is used to prevent artificial reflection from the edge of the grid. Propagation in time is achieved by the split-operator technique which is an $\mathscr{O}(\Delta t^3)$ approximation in the time step Δt [46]. Typically, a time step of $\Delta t = 1\hbar/E_h$ (atomic units: 1 $E_h = 27.21112$ eV) was chosen.

Time-dependent populations of bound states are obtained by projection of the non-stationary wavefunctions $\psi_g(t)$ or $\psi_e(t)$ on the $n_g = 17$ or $n_e = 11$ bound vibrational states v_g or v_e of the respective potential

$$P_{v_{g,e}}(t) = |\langle v_{g,e}|\psi_{g,e}(t)\rangle|^2, \quad 0 \le v_{g,e} \le (n_{g,e} - 1). \quad (8)$$

The vibrational eigenenergies and eigenfunctions are computed for both electronic states by the Fourier grid Hamiltonian method [47]. Accordingly, the total population of all the bound states of the potential well and the total population of continuum states are given by

$$P_{well_{g,e}}(t) = \sum_{v_{g,e}=0}^{n_{g,e}-1} P_{v_{g,e}}(t),$$
$$P_{cont_{g,e}}(t) = \int_{\Delta r}^{N\Delta r} |\psi_{g,e}(r,t)|^2 \, dr - P_{well_{g,e}}(t) \quad (9)$$

for ground (g) or excited (e) electronic state. The state selectivity

$$S_{v_{g,e}}(t) = P_{v_{g,e}}(t)/P_{well_{g,e}}(t) \quad (10)$$

is used to characterize the preparation of molecules in a specific $|v_{g,e}\rangle$ bound state.

3. Results

3.1. Initial wavepackets

As has been shown in our previous studies, the investigation of laser induced photodissociation [48,36] yields valuable information for the understanding of the reversed process of photoassociation using similar laser pulses. In a first series of simulations we study the photodissociation for different bound electronic states of the OH molecule. Fig. 2 shows the population of various states after excitation of an arbitrarily chosen bound state with an ultrashort laser pulse of duration $\tau = 0.5$ ps and amplitude $\mathscr{E}_0 = 0.07$ $E_h/(ea_0)$ (atomic units: $1E_h/(ea_0) = 5.1422 \times 10^{11}$ V/m) versus the carrier frequency ω of the pulse. For case (a), the initial state is the $v_g = 12$ vibrational level of the electronic ground state (for a remark on other vibrational states, see the Discussion). For a linear polarization of the external laser fields along the x axis, one recognizes the signature of excitation to the top vibrational level $v_g = 16$ just below the dissociation limit of the ground state potential. Beyond this threshold there is a sudden rise of the continuum population at $\omega \approx 4050$ cm^{-1}. The photodissociation yield is approximately constant up to $\omega \approx 4800$ cm^{-1}. For higher frequencies, there are a few dips corresponding to transitions

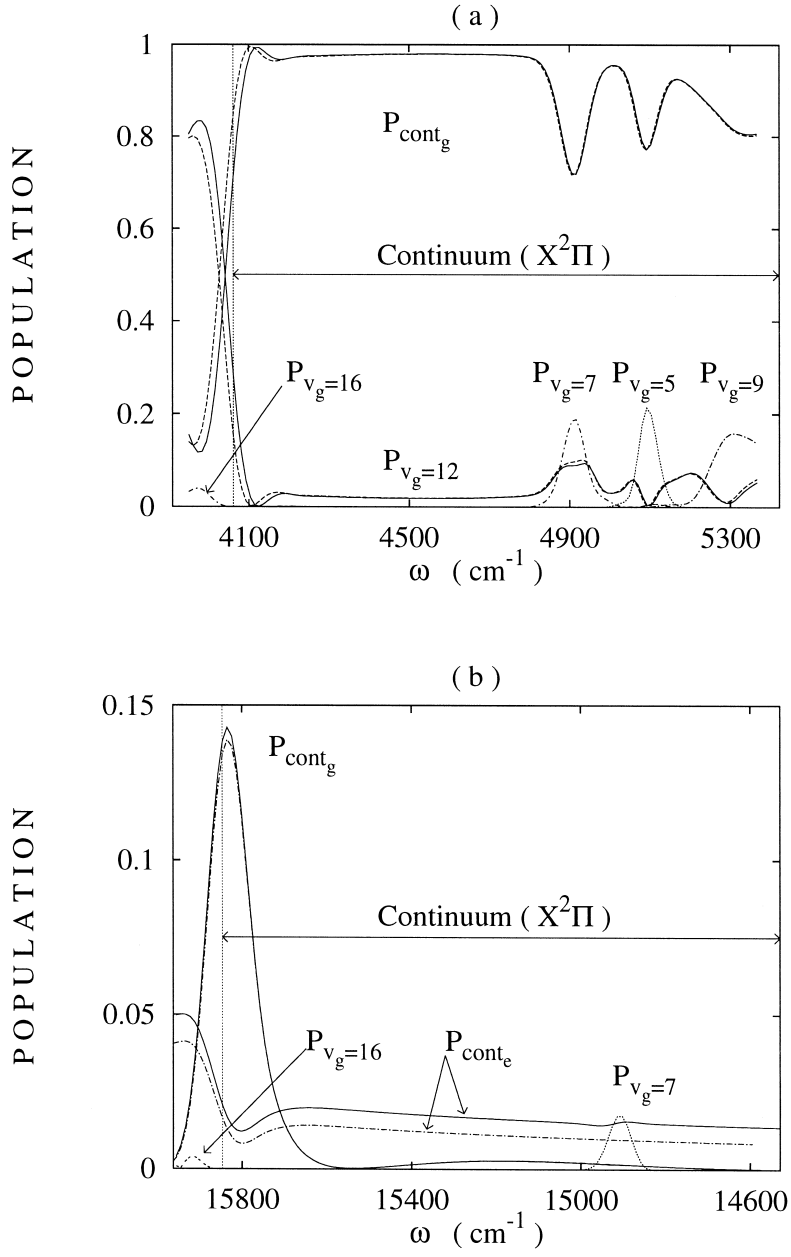

Fig. 2. Population of bound and continuum states after excitation of a bound state of the OH molecule with an ultrashort laser pulse ($\tau = 0.5$ ps, $\mathscr{E}_0 = 0.07E_h/(ea_0)$) as a function of the carrier frequency ω for two different initial states. (a) $v_g = 12$, electronic ground state. (b) $v_e = 10$, top level of the excited electronic state (note the reversed abscissa). In either case, the population P_{cont} of continuum states gives the photodissociation yield while populations of bound states P_v indicate various bound $\leftarrow$ bound transitions. The vertical dotted lines and the horizontal arrows indicate the dissociation threshold of the ground ($X^2\Pi$) state. The solid curves show the result for synchronous x and z polarization, the dashed curves in part (a) for x polarization, the dot-dashed curves in part (b) for z polarization.

down to lower vibrational states by stimulated emission of one (e.g. $v_g = 9 \leftarrow v_g = 12$), two ($v_g = 7$), or three (e.g. $v_g = 5$) photons. Close to the respective resonance frequencies, the competition with these transitions reduces the photodissociation yield down to approximately 70 . . . 80%. In principle, the branching ratio can be controlled by variation of the field amplitude $\mathscr{E}_0$.

Although there is no considerable population of the excited electronic state there is a signature of this process. Including a *z*-polarization (perpendicular to the molecular axis) of the external fields shifts the dissociation threshold towards slightly higher frequencies (see solid curves). For a more detailed discussion of these shifts, see below.

The situation changes completely when considering laser pulse-induced transitions from a bound OH molecule in the excited electronic state. For reasons explained below, the initial state is assumed to be the top vibrational level $v_e = 10$. Assuming a light polarization along the *z*-axis, we first consider photodissociation of this state to yield fragments $O(^3P) + H(^2S)$ in the electronic ground state which proceeds via stimulated emission. Fig. 2(b) shows that the population of these continuum states exhibits the following behavior: First, there is a strong peak at energies around $\omega \approx 15835\ \mathrm{cm}^{-1}$ which is just above the dissociation threshold of the ground state. The resulting photofragments are very slow with $K_0 \approx 0.423\ \mathrm{a}_0^{-1}$ corresponding to fragment energies of about $E_0 = 11\ \mathrm{cm}^{-1}$. Due to the weak transition dipole moment $\mu_{g,e}$ for $r \geq 1.5\ \mathrm{a}_0$, the maximum yield of 14% for the sharp peak is considerably lower than for photodissociation of ground state molecules. Second, there is a very broad feature centered around $15200\ \mathrm{cm}^{-1}$ which is substantially weaker ($P_{\mathrm{cont}_g} = 0.2\%$). It is noted, that for all lower vibrational states ($v_e < 10$) the yield is even considerably less because for those states the region of maximum probability amplitude comes close to the root of the transition dipole moment $\mu_{g,e}$ at $r = 2.64\ \mathrm{a}_0$ (see Fig. 1b).

Fig. 2(b) also shows bound $\leftarrow$ bound transitions to the electronic ground state induced by stimulated emission of one ($v_g = 16 \leftarrow v_e = 10$) or two ($v_g = 7$) photons. Moreover, the stimulated emission processes compete with the absorption process reaching the continuum of the electronically excited state. This photodissociative event yields a pair of fragments with electronically excited oxygen atoms $O(^1D) + H(^2S)$. Due to the typical behavior of continuum $\leftarrow$ bound transitions (see Ref. [49] and Fig. 3(c) of Ref. [36]), the corresponding continuum population P_{cont_e} is relatively low (1 . . . 2%) and it smoothly decreases with increasing ω. It is interesting to note that this process is also observed for the case of vanishing *x* polarization of the laser field (dot-dashed curve) thus suggesting a ''down-up'' two-photon process via the continuum of the electronic ground state. Again note that the competition between these processes is a function of the field $\mathscr{E}_0$.

Based on these considerations of the fragment energies of the photodissociating OH molecule, we can already predict the dependence of the photoassociation yield versus momentum K_0 of the incident wavepacket. Apart from the multi-photon processes (e.g. $v_g = 5,7,9$ in Fig. 2(a)) the yield of the ground state reaction can be expected to be a relatively smooth function of K_0. In contrast, the yield for the excited state process is very sensitive to the choice of K_0 (see Fig. 2(b)). It will be enough effective only for very slow collision pairs with $0 < E_0 < 100\ \mathrm{cm}^{-1}$. Unless stated otherwise, we will restrict ourselves in the following to wavepackets with incident momenta of $K_0 = -0.7\ \mathrm{a}_0^{-1}$ ($E_0 = 31.1\ \mathrm{cm}^{-1}$, near the center of the sharp peak in Fig. 2(b)) and $K_0 = -3.5\ \mathrm{a}_0^{-1}$ ($E_0 = 777.7\ \mathrm{cm}^{-1}$, near the center of the broad peak in Fig. 2(b)) as initial states for the photoassociation processes under investigation. It is noted that due to the time-dependence of the electric field as well as of in- and outgoing wavepackets, this sensitivity analysis is not an exact analogue to just considering (stationary) Franck-Condon factors.

As in our previous study of ground state photoassociation [34], the next step of our work is to study elastic collisions of ground state O + H collision pairs in the time-dependent wavepacket picture ($\mathscr{E}_0 = 0$) in order to learn about the time scales of these processes. The initial state is specified by Eq. (4) with the above-mentioned initial momenta. The two atoms are assumed to be initially at an average distance of $\langle r \rangle = r_0 = 25\ \mathrm{a}_0$ which is well outside the interaction region. The relatively large value for the uncertainty in the distance coordinate $\Delta r = a/2$ with $a = 10\ \mathrm{a}_0$ ensures a small momentum spread of $\Delta k = 1/a = 0.1\ \mathrm{a}_0^{-1}$ thus modeling high quality

beam experiments [50]. After 1.15 ps ($K_0 = -0.7$ a_0^{-1}) or after 0.25 ps ($K_0 = -3.5$ a_0^{-1}) the wavepacket has reached the interaction region with its center at its reflection point. Fig. 3 shows the interference of ingoing and outgoing parts of the wavepacket. In the asymptotic region of the potential the nodal pattern with distances of $\Delta R = \pi/K_0$ is resembling a standing wave but with different ampli-

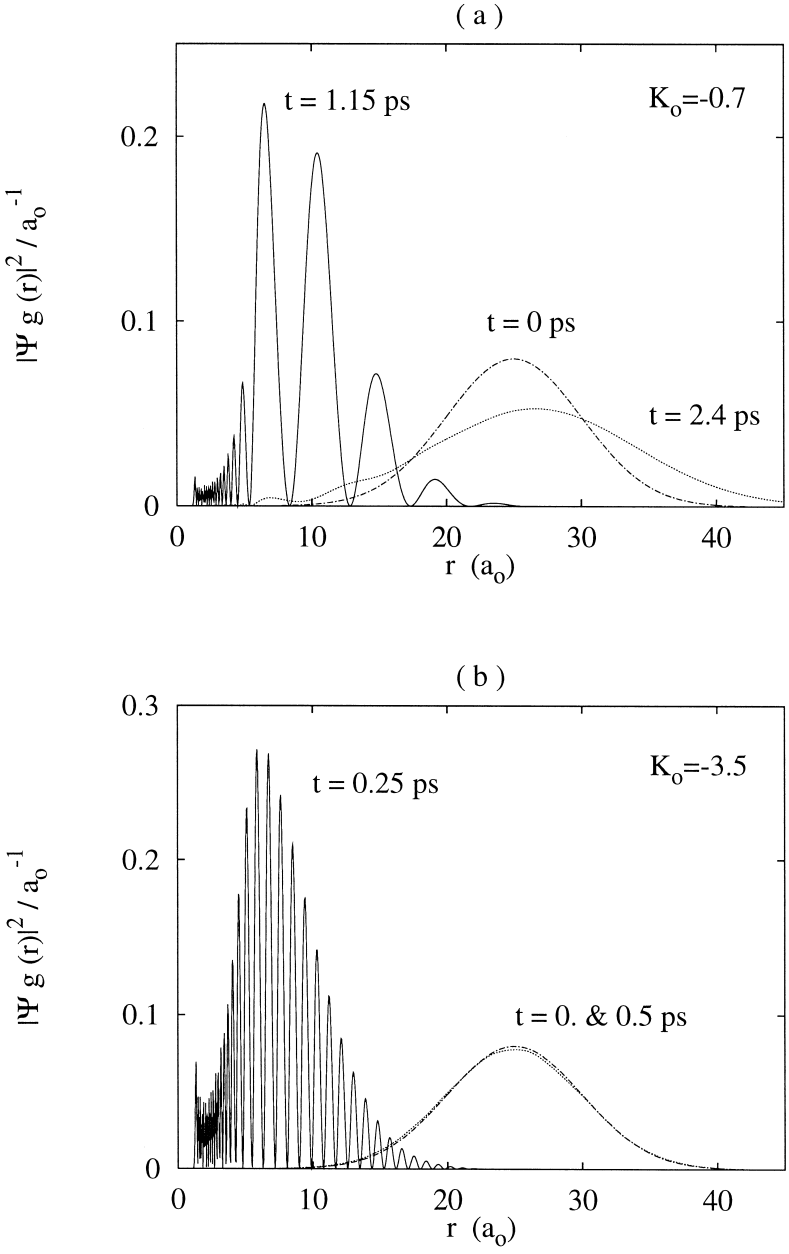

Fig. 3. Elastic scattering of a wavepacket in the electronic ground state for two different scattering energies (momenta), see Eq. (4). (a) $E = 31.1$ cm^{-1} ($K_0 = -0.7$ a_0^{-1}). (b) $E = 778$ cm^{-1} ($K_0 = -3.5$ a_0^{-1}). In either case, the dot-dashed and the dotted curve show initial and final state of the scattering event, respectively. The solid curve shows the intermediate (transition) state.

tudes (see also Refs. [34,33]). After twice this time, the wavepacket has returned to the initial position. Note that for the low energy case, there is already a considerable spread of the wavepacket in coordinate space.

This investigation of the passing of wavepackets through the interaction region of a collision where both potentials and (transition) dipole moments are non-vanishing is helpful to determine two quantities: First, the timescale of the collision event can be used to determine the duration of the laser pulses most suitable to manipulate the collision pair. Here we will always use laser pulses with a duration between $\tau = 0.5$ ps and $\tau = 1.5$ ps. Second, the time delay δt between the start of the incident wavepacket and the beginning of the laser pulse can be roughly estimated.

3.2. Ground state photoassociation

Assuming all the parameters of the initial wavepacket of Eq. (4) and the timing information as given above, the next task is to optimize the laser pulses of Eq. (7) in order to achieve optimal yield for photoassociation products. We use an optimization method similar to Ref. [51], together with an optimization of the relative timing of collision event and laser pulse [34]. In particular, our free parameters are the frequency ω, the amplitudes $\mathscr{E}_x$ and (or) $\mathscr{E}_z$ of the electric field, and the time delay δt of the laser pulse. Results of these optimizations are shown in Fig. 4. Part (a) and (b) show the yield of OH molecules in the $v_g = 12$ target level of the electronic ground state for different initial momenta K_0. First we want to discuss the results for x-polarization of the field only, see dashed curves. In the low energy case ($K_0 = -0.7$ a_0^{-1}) there is one peak centered near the resonance frequency $\omega_{res,1} = (E_0 - E_{v_g=12})/\hbar$ of the bound $\leftarrow$ free transition (see Fig. 4(a)). For a field strength of $\mathscr{E}_0 = 0.0315 E_h/(ea_0)$ the height of the peak indicates a good efficiency of $P_{well_g} = 71.2\%$ for this process. At the same time, the selectivity is very high ($S_{v_g=12} > 99.5\%$). For the higher initial energy ($K_0 = -3.5$ a_0^{-1}) the photoassociation reaches a slightly higher yield of $P_{v_g=12} = 85.6\%$ but at higher fields ($\mathscr{E}_0 = 0.0709 E_h/(ea_0)$, see Fig. 4(b)). However, the selectivity is reduced to $S_{v_g=12} = 95.1\%$ and the main peak of the spectrum is considerably red-shifted by approximately 40 cm^{-1} with respect to the resonance frequency $\omega_{res,1}$. This may be a consequence of a nearby three-photon resonance $\omega_{res,2} = (E_0 - E_{v_g=7})/(3\hbar)$ which also causes the shoulder at the high energy edge of the peak, see Fig. 4(b).

It is obvious that the competition between the one-photon transition down to $v_g = 12$ and the three-photon transition down to $v_g = 7$ can be controlled by changing the momentum of the incident wavepacket. Fig. 5 shows our results for a relatively narrow interval around $K_0 = -3.5$ a_0^{-1}. For $K_0 = -3.22$ a_0^{-1} the two peaks are further separated and can be clearly distinguished. On the contrary, for $K_0 = -3.72$ a_0^{-1} the two resonance frequencies $\omega_{res,1}$ and $\omega_{res,2}$ are nearly coincident. As a consequence, the three-photon process causes a dip in the curve giving the yield of $P_{v_g=7}$ for the one-photon process.

3.3. Frequency shifts

In the following we want to discuss the influence of coupling to the excited electronic state on the quantum dynamics of the ground state photoassociation as illustrated in Figs. 4(a) and (b). This can be seen from the difference of the simulations for x-polarized light (dashed curves) and simulations where an additional z-polarization of the external field couples the ground to the excited state dynamics (see solid curves). Although the frequency range around 4000–5000 cm^{-1} is not suitable to populate the excited electronic state notably (unfavorable transition dipole moment $\mu_{g,e}(r)$, see Fig. 1(b)), the presence of the excited state can nevertheless be detected from a small but characteristic blue shift of about $\Delta\omega \approx 3.4$ cm^{-1} ($K_0 = -0.7$ a_0^{-1}) or $\Delta\omega \approx 15.5$ cm^{-1} ($K_0 = -3.5$ a_0^{-1}).

It is straight-forward to explain these blue-shifts at least qualitatively in a ''dressed molecule'' picture [52,53]. Shifting up the ground state potential by the energy of one photon and then coupling it by the semiclassical expression to the excited state potential gives the potential energy in a diabatic representation

$$\mathbf{V}(r) = \begin{pmatrix} V_g(r) + \hbar\omega & -\mu_{g,e}(r)\,\mathscr{E}_0/2 \\ -\mu_{g,e}(r)\,\mathscr{E}_0/2 & V_e(r) \end{pmatrix}.$$

Diagonalization yields adiabatic potential curves $V_1(r)$ and $V_2(r)$ representing light-induced effective

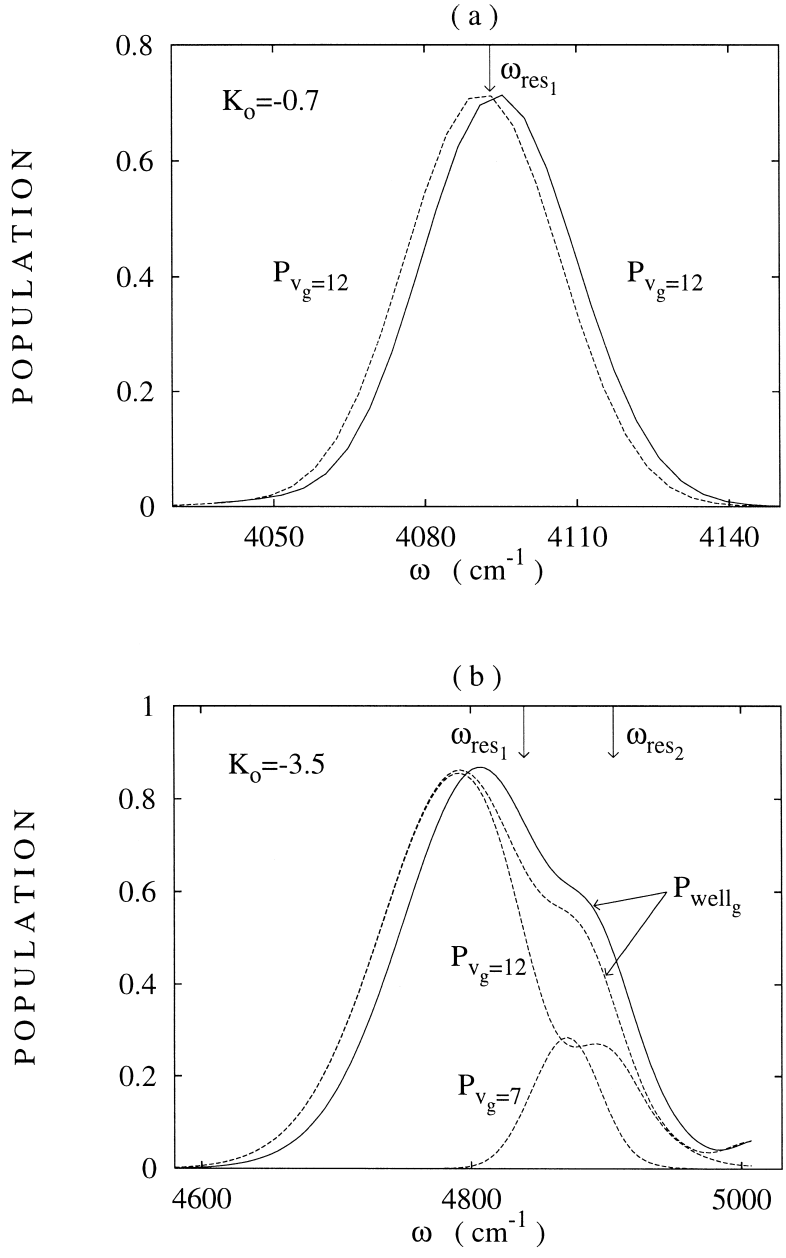

Fig. 4. Photoassociation yield in the electronic ground state versus frequency ω of the infrared laser pulse. The curves show the bound state population at the end of the laser pulse. The solid curves show the result for synchronous x and z polarization, the dashed curves for x polarization only. (a) For lower scattering energy ($K_0 = -0.7\ a_0^{-1}$, $\tau = 1.5$ ps, $\mathscr{E}_0 = 0.0315 E_h/(ea_0)$). (b) For higher scattering energy ($K_0 = -3.5\ a_0^{-1}$, $\tau = 0.5$ ps, $\mathscr{E}_0 = 0.0709 E_h/(ea_0)$). The arrows at the top indicate the one- and three-photon resonance frequencies $\omega_{\mathrm{res},1} = (E_0 - E_{v_g=12})/\hbar$, $\omega_{\mathrm{res},2} = (E_0 - E_{v_g=7})/(3\hbar)$.

potential curves in the presence of a periodic field continuously oscillating with a frequency ω. Note that the pulse shape (7) is replaced by a time-averaged amplitude $\mathscr{E}_0/2$. For the low frequencies and moderate fields considered here, there are no (avoided) crossings which could lead to the typical

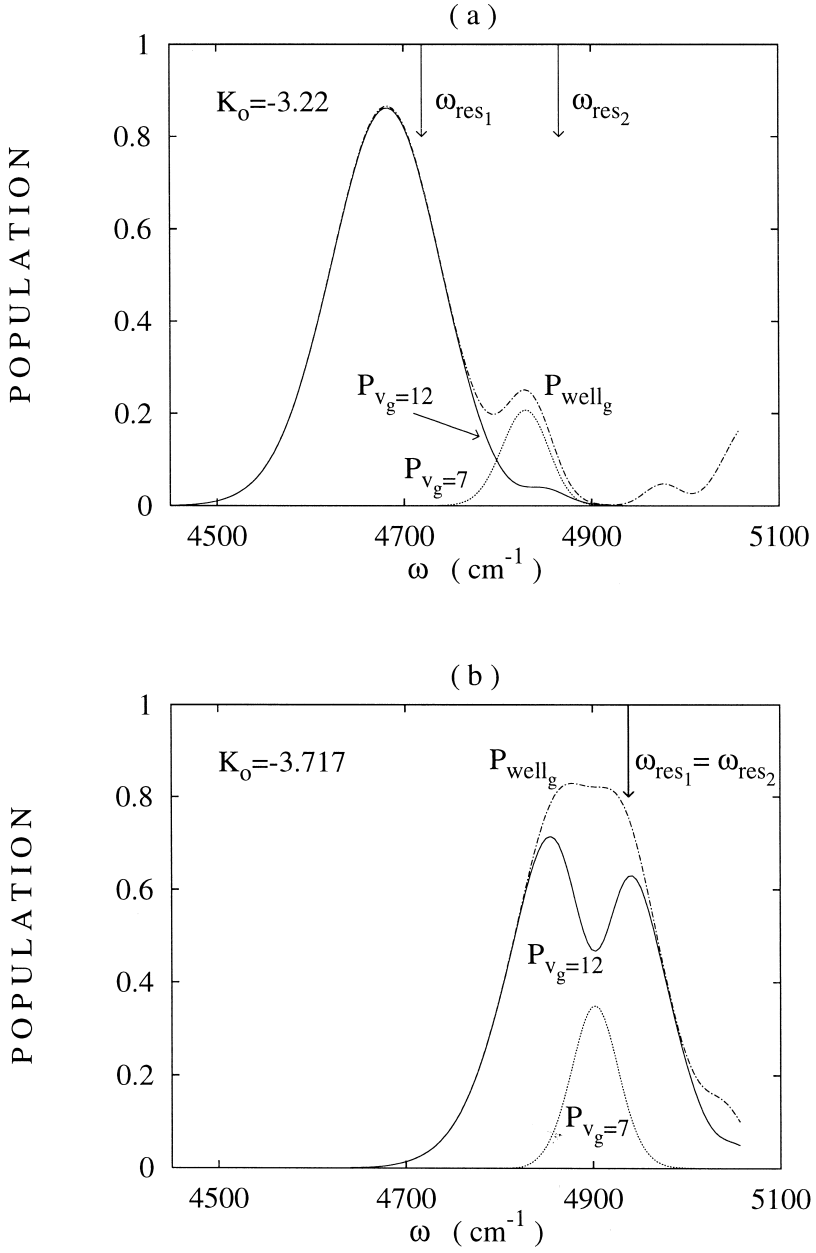

Fig. 5. Same as Fig. 4(b), but for slightly varied values of the initial momentum K_0 (for $\tau = 0.5$ ps, $\mathscr{E}_x = 0.0709 E_h/(ea_0)$) and for x-polarization only. (a) Larger distance of the resonance frequencies $\omega_{\mathrm{res},1}, \omega_{\mathrm{res},2}$ for $K_0 = -3.22\ \mathrm{a}_0^{-1}$. (b) Nearly coinciding resonance frequencies $\omega_{\mathrm{res},1}, \omega_{\mathrm{res},2}$ for $K_0 = -3.72\ \mathrm{a}_0^{-1}$.

strong-field effects discussed in the literature [52,53]. However, we find a small increase or decrease in the well depth of V_1 or V_2, respectively. Hence, the ''dressed'' vibrational energy levels of the lower adiabatic state V_1 are lowered which results in a blue shift $\Delta E_{v_1} > 0$ of transitions from or to the dissociation threshold $V_1(r \to \infty) = V_g(r \to \infty) + \hbar\omega$ (see Fig. 6). For a typical frequency of $\omega \approx 4400\ \mathrm{cm}^{-1}$, the

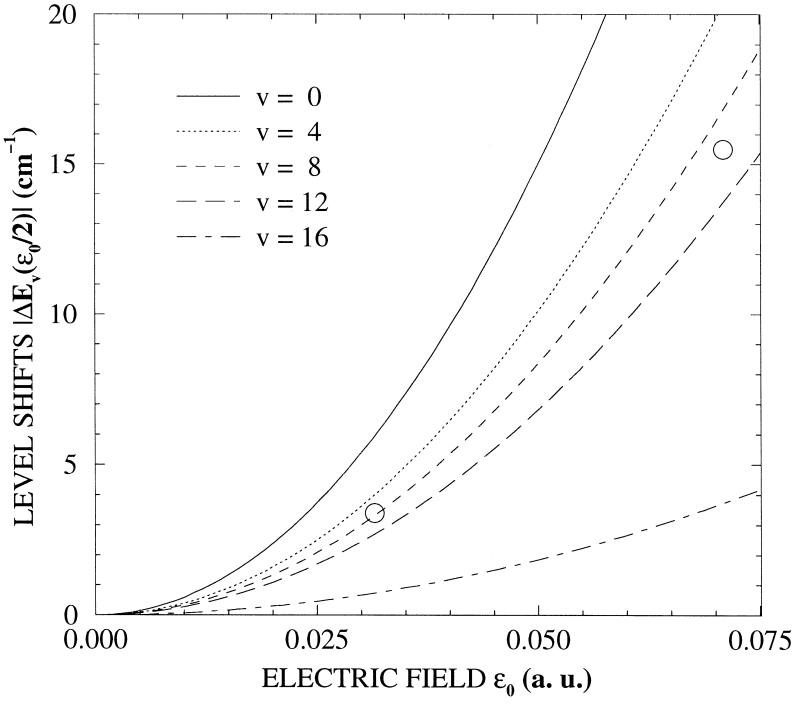

Fig. 6. Shifts of vibrational energy levels of the lower electronic state $V_1(r)$ in the ''dressed molecule'' picture. The curves show the absolute shifts $|\Delta E_{v_1}|$ for various vibrational levels with respect to the dissociation threshold versus electric field (for $\omega = 4390$ cm^{-1}). The open circles indicate the frequency shifts $\Delta E_{v_1=12}$ obtained from Fig. 4(a) and (b).

shift $\Delta E_{v_1=12}$ of the 12-th state indeed is very close to our numerically exact values (see above) obtained from the coupled Schrödinger equations and for the realistic pulse shape. Note that all of these shifts are much larger than the frequency shifts associated with the spin-orbit induced Λ-doubling for the electronic ground state of the OH molecule which is in the order of only 0.1 cm^{-1} [54].

3.4. Excited state photoassociation

Now we want to discuss transitions from the continuum of the electronic ground state to the excited electronic state of the OH molecule induced by visible light. This process is illustrated in Fig. 7(a) for the case of low scattering energy ($K_0 = -0.7$ a$_0^{-1}$). Here frequencies and electric fields are varied in order to optimize the population of the top level ($v_e = 10$) of the excited electronic state at the end of the laser pulse. First, let us consider the case of z-polarization only (dot-dashed curves). Even for very intense fields ($\mathscr{E}_0 = 0.16 E_h/(ea_0)$), this level can only be populated up to $P_{v_e=10} = 29\%$, but at extremely high selectivity ($S_{v_e=10} > 99.99\%$). At slightly higher frequencies, there is an onset of dissociation in the excited ($A^2\Sigma^+$) state yielding considerable population $P_{\mathrm{cont_e}}$ of the continuum of the excited electronic state. These states correspond to the re-dissociation of collision pairs yielding electronically excited oxygen atoms O(^{1}D) + H(^{2}S). Note that the maximum of the photoassociation probability $P_{v_e=10}$ at 15868 cm^{-1} is considerably shifted towards higher frequencies (52 cm^{-1}) with respect to the resonance frequency $\omega_{\mathrm{res}} = E_{v_e=10} - E_0$. Analogously, the onset of $P_{\mathrm{cont_e}}$ is blue-shifted with respect to the dissociation threshold of the excited state. For additional x polarization of the electric field, the peaks for the bound $\leftarrow$ continuum and for the continuum $\leftarrow$ continuum are only slightly shifted ($\Delta\omega \approx 4$ cm^{-1}).

As anticipated previously, the process of electronic excitation becomes far less effective for higher

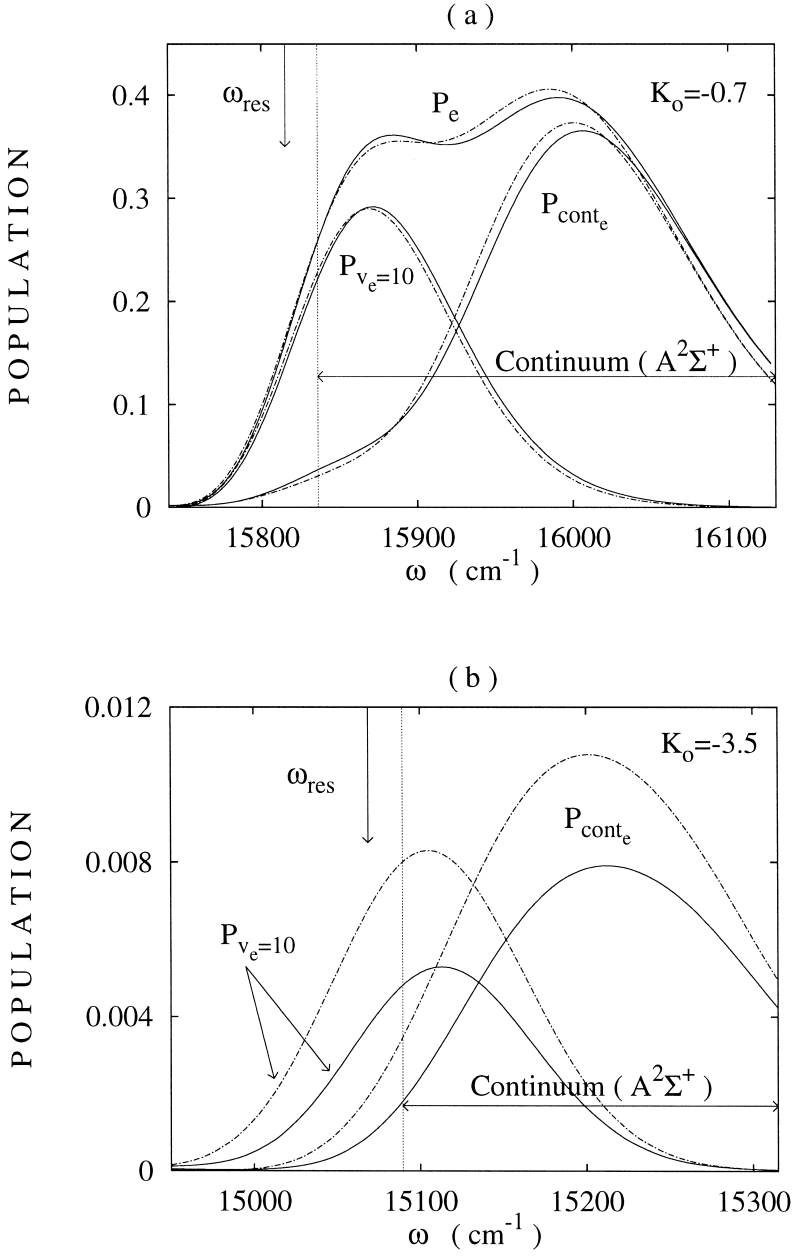

Fig. 7. Photoassociation yield in the excited electronic state versus frequency ω of the visible laser pulse. (a) For low scattering energy ($K_0 = -0.7\ a_0^{-1}$, $\tau = 1.5$ ps, $\mathscr{E}_0 = 0.16 E_h/(ea_0)$). (b) For high scattering energy ($K_0 = -3.5\ a_0^{-1}$, $\tau = 0.5$ ps, $\mathscr{E}_0 = 0.18 E_h/(ea_0)$). The curves show the population of the highest bound state ($P_{v_e=10}$), the population of continuum states ($P_{\mathrm{cont_e}}$), and the total population P_e of the electronically excited state. Vertical arrows indicate the resonance frequency $\omega_{res} = (E_{v_e=10} - E_0)/\hbar$, horizontal arrows indicate the dissociation limit of the excited state. Dot-dashed curves: z-polarization only, solid curves: x and z polarization.

initial energy of the incoming wavepacket. This is shown in Fig. 7(b) for an initial momentum of $K_0 = -3.5\ a_0^{-1}$. The yield is in the regime of only 1% even for very high fields ($\mathscr{E}_0 = 0.182 E_h/(ea_0)$). In this case there is a strong difference between the heights of the peaks for z-polarization only and those

for simultaneous x and z-polarization. It can be seen from the solid curves that the population of bound and continuum levels of the electronically excited state is substantially reduced for the latter case. This is a signature of either free ← free or bound ← free transitions within the electronic ground state. The blue-shift $\Delta\omega = 8.8\ \mathrm{cm}^{-1}$ is larger than for the previous case.

As demonstrated above, the direct pathway for excited state photoassociation associated with absorption of one photon is not very effective for realistic values of the electric field. In order to overcome these limitations, we suggest another way to excited state photoassociation by a sequence of two laser pulses. The proposed two-pulse ''dump-pump'' strategy consists of the following two steps. A first ''dump'' laser pulse is used to associate the collision pair in the electronic ground state. Then a second ''pump'' laser pulse can induce a vibrationally state-selective bound ← bound electronic transition as discussed in Ref. [38]. First, let us consider the case for low collision energy ($K_0 = -0.7\ \mathrm{a}_0^{-1}$). The corresponding population dynamics is shown in Fig. 8. As has been discussed previously, an optimized ''dump'' pulse ($\tau = 1.5$ ps, $\omega = 4093.2\ \mathrm{cm}^{-1}$, $\mathscr{E}_z = 0.0315 E_h/(ea_0)$) can transfer $P_{\mathrm{well_g}} = 71.4\%$ of the wavepacket into bound states of the well, see also Fig. 4(a). The vibrational state selectivity of this process at the end of the laser pulse is very high ($S_{v_g=12} > 99.5\%$). After the first pulse, a second optimized laser pulse ($\tau = 1$ ps, $\omega = 19907\ \mathrm{cm}^{-1}$, $\mathscr{E}_z = 0.018\, E_h/(ea_0)$) is used to induce the bound ← bound electronic transition. In this case the overall excitation efficiency is much higher than in the direct association process. We find a value of ($P_e = 71.3\%$) with $P_{\mathrm{well_e}} = 68.2\%$ being transferred to the bound states of the well and $P_{\mathrm{cont_e}} = 3.1\%$ re-dissociating into the excited electronic continuum. The bound state population is found exclusively in the specified $v_e = 10$ target state.

Our results for the case of higher scattering energy ($K_0 = -3.5\ \mathrm{a}_0^{-1}$) are shown in Fig. 9. A first laser pulse dumps $P_{\mathrm{well_g}} = 86.6\%$ into the bound states of the well. This population is transferred by a second pulse with only marginal losses to the well of the electronically excited state ($P_{\mathrm{cont_e}} = 82.5\%$). Again, the state selectivity is extremely close to unity ($S_{v_e=10} > 99.99\%$). In this case the gain in

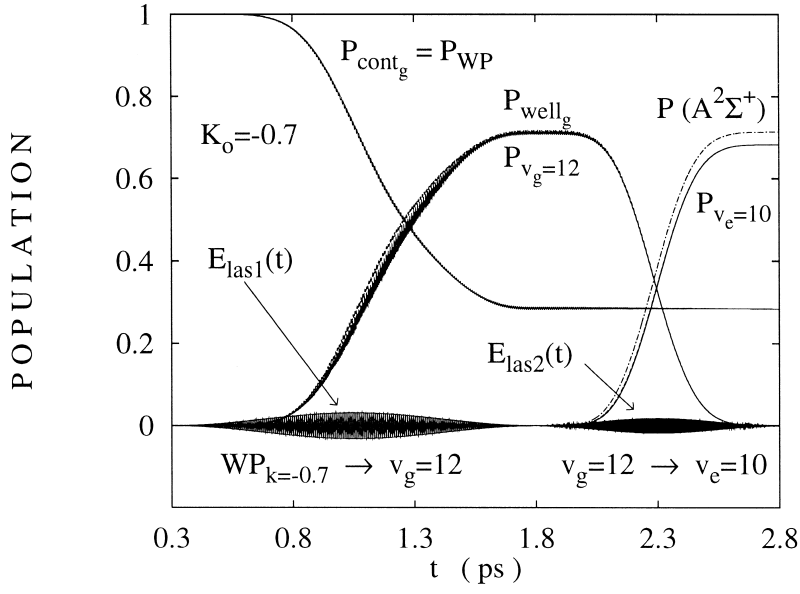

Fig. 8. Population dynamics for the excited state photoassociation using a two-pulse ''dump-pump'' strategy for low scattering energy ($K_0 = -0.7\ \mathrm{a}_0^{-1}$). The first (''dump'') pulse ($\tau = 1.5$ ps, $\omega = 4093.2\ \mathrm{cm}^{-1}$, $\mathscr{E}_x = 0.0315 E_h/(ea_0)$, see also Fig. 4(a)) populates the $v_g = 12$ level, the second (''pump'') pulse excites the OH molecule to the $v_e = 10$ level ($\tau = 1.0$ ps, $\omega = 19907\ \mathrm{cm}^{-1}$, $\mathscr{E}_z = 0.018\, E_h/(ea_0)$).

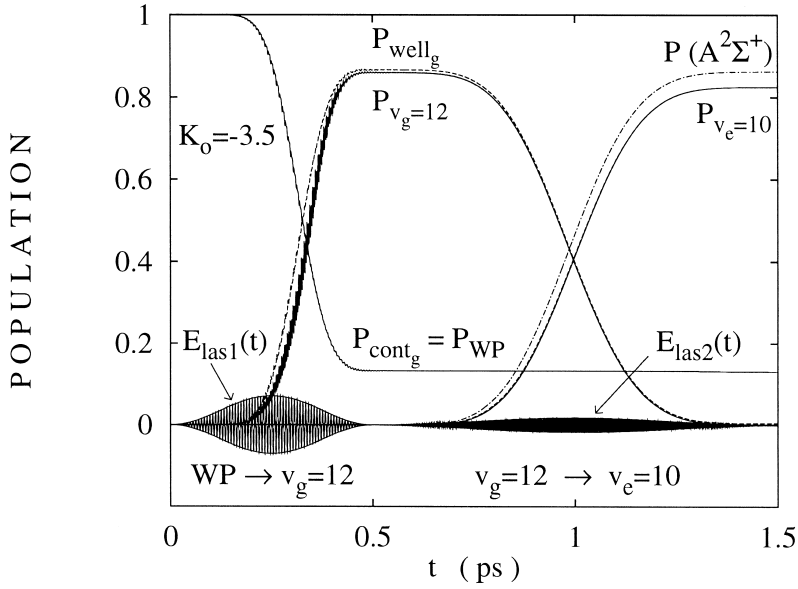

Fig. 9. Same as Fig. 8, but for higher scattering energy ($K_0 = -3.5\ a_0^{-1}$) and with different parameters of the first (''dump'') pulse ($\tau = 0.5$ ps, $\omega = 4792.2\ cm^{-1}$, $\mathscr{E}_x = 0.0709 E_h/(ea_0)$, see also Fig. 4(b)).

efficiency is beautifully demonstrated. Compared with the direct process using a single pulse as illustrated in Fig. 4(b), the yield P_{v_e} increases by more than two orders of magnitude.

The ''dump-pump'' strategy proposed here can be regarded as a complementary approach to the work of Vardi et al. on the sodium dimer [32]. In order to achieve photoassociation in the ground state for a system with a vanishing dipole moment $\mu_g(r) = 0$ these authors suggest a ''pump-dump'' strategy: First a collision pair is pumped to an excited electronic state and then it is dumped to vibrational levels of the ground state again.

4. Discussion

This work presents a study of ground and excited state photoassociation processes for a model of the hydroxyl molecule comprising of two bound electronic states. In principle there are two pathways to form bound OH molecules from a ground state collision pair $O(^3P) + H(^1S)$. The first one is the stimulated emission of light yielding molecular products in the electronic ground state. It is demonstrated that by optimizing laser pulses in the picosecond regime this reaction can be made very effective with quantum yields of $P_{well_g} > 80\%$ for scattering energies around 1000 cm^{-1} (≈ 100 meV) which is typical for atomic beam experiments [50]. For the example of the $v_g = 12$ state it is shown that the vibrational state selectivity can be very close to $S_{v_g} = 100\%$ unless there is a near coincidence with two- (or more) photon transitions to lower bound states, see also Ref. [35]. The latter case, however, can be easily avoided by carefully choosing scattering versus photon energy. Note that we have obtained similar results for other vibrational levels ($12 < v_g < 16$), as well. However, when trying to populate lower vibrational states, there is a principal limitation. Due to the lower anharmonicity, the Franck-Condon factors are decreasing, and correspondingly increasing electric fields are necessary. However, in analogy to previous results on excitation of vibrational states [36,48], photoassociation with the very lowest vibrational states as target levels can be achieved more effectively by a sequence of infrared laser pulses.

The effect of laser-induced transitions to the excited electronic state manifests itself in small but characteristic blue shifts in the spectra for ground state photoassociation. These shifts can be qualitatively explained using adiabatic potential curves in

the ''dressed molecule'' picture assuming a continuous light source. However, for an exact description, the coupled Schrödinger equations have to be solved for the realistic pulse shapes.

The second pathway to permanent association is the excitation of the O + H collision pair by absorption of light to a bound excited state. In general it is found that photoassociation to the excited electronic state of the OH molecule is considerably less effective and is only possible for the top vibrational level $v_e = 10$. As a consequence of the close proximity of the top level to the dissociation threshold, the total yield of population of the well is notably reduced because it competes with re-dissociation in the continuum of the excited electronic state. Furthermore, as a result of unfavourable Franck-Condon factors the association yield is only non-vanishing for extremely low scattering energies which can be realized rather in laser cooling experiments than in conventional beam experiments. Of course, the observed behaviour of the excited state photoassociation originates from the peculiarities of the transition dipole moment for the $A^2\Sigma^+ \leftarrow X^2\Pi$ transition of the OH molecule, see Fig. 1(b). For other molecules with larger transition dipole moments $\mu_{g,e}(r)$ photoassociation in the excited state may be a far more effective process.

An alternative way to overcome the low efficiency of the excited state photoassociation process is also outlined in the present work. We suggest a two-pulse ''dump-pump'' strategy where the first laser pulse dumps the system into a bound level of the electronic ground state and a second laser pulse excites the system to the higher electronic state. Applying this procedure, the efficiency is mostly limited by the first step yielding in the order of $P_{\mathrm{well}_e} \approx 80\%$. A very high vibrational state selectivity close to $S = 100\%$ can be achieved. In addition, lower vibrational states ($v_e < 10$) can be populated, too.

In the present one-dimensional model the effect of collisions with non-vanishing impact parameter leading to rotation of the molecular association product has been neglected. However, in recent work we have shown that highly state selective photoassociation in the electronic ground state can also be achieved for collision pairs with non-zero angular momenta [37]. In another study it is shown that the high efficiency of the population transfer ($P \approx 100\%$) can also be achieved for rotating molecules [55].

Finally, the results obtained for single pulse photoassociation open several ways of controlling the branching ratio of ground and excited state photoassociation for the O + H collision pair. (i) The restriction of the excited state process to the $v_e = 10$ level strongly restricts the range of carrier frequencies to a narrow interval around $15700 \ldots 16100$ cm^{-1}, see Fig. 7. Since this is far off resonance for bound $\leftarrow$ free transitions in the ground state, and also the efficiency for free $\leftarrow$ free transitions is negligible, molecules can be formed only in the excited electronic state. On the other hand, the low frequency regime suitable for ground state photoassociation ($\omega = 4000 \ldots 5000$ cm^{-1}, see Figs. 4,5) is only eligible for excited state photoassociation for low values of v_e which, however, is not efficient. (ii) The strong dependence on the initial scattering energy can also be used to control the electronic branching ratio. Because excited state photoassociation is only effective for very slow collision energies, this process can be excluded for collision pairs with higher initial momenta. (iii) Finally, due to the different orientation of permanent and transition dipole moments, the dynamics of the photoassociation reaction of oriented molecules can also be controlled via the polarization of the light pulses.

The present results are for a model situation where timing, position, and width of the incoming wavepacket can be controlled. This can perhaps be realized in an experiment where the collision event is preceded by photodissociation of a geometrically confined precursor complex induced by a laser pulse. However, in other situations the timing of the collision event versus the laser pulse can be less perfect, and the photoassociation yield will be reduced. But even for the much less favorable situation of a gas at ambient temperature, it was already shown that photoassociation spectroscopy using femtosecond pulses is indeed feasible [26]. Hence, the present exploratory study may serve as a guideline for future experiments.

Acknowledgements

Financial support by the Deutsche Forschungsgemeinschaft (DFG) through grant Ma 515/14-2 is

gratefully acknowledged. Furthermore, we would like to thank J. Manz for stimulating discussions. The computer simulations were carried out on a Hewlett-Packard workstation cluster at the Freie Universität Berlin.

References

[1] A.H. Zewail (Ed.), Femtochemistry – Ultrafast Dynamics of the Chemical Bond, World Scientific, Singapore, 1994.
[2] J. Manz, L. Wöste (Eds.), Femtosecond Chemistry, Verlag Chemie, Weinheim, 1995.
[3] M. Chergui (Ed.), Ultrafast Chemical and Physical Processes in Molecular Systems, World Scientific, Singapore, 1996.
[4] V. Sundstroem (Ed.), Femtochemistry and Femtobiology, World Scientific, Singapore, 1997.
[5] T. Sizer, M.G. Raymer, Phys. Rev. A 36 (1987) 2643.
[6] H.R. Thorsheim, J. Weiner, P.S. Julienne, Phys. Rev. Lett. 58 (1987) 2420.
[7] P.D. Lett, K. Helmerson, W.D. Phillips, L.P. Ratliff, S.L. Rolston, M.E. Wagshul, Phys. Rev. Lett. 71 (1993) 2200.
[8] L.P. Ratliff, M.E. Wagshul, P.D. Lett, S.L. Rolston, W.D. Phillips, J. Chem. Phys. 101 (1994) 2638.
[9] C.J. Williams, P.S. Julienne, J. Chem. Phys. 101 (1994) 2634.
[10] P.D. Lett, P.S. Julienne, W.D. Phillips, Annu. Rev. Phys. Chem. 46 (1995) 423.
[11] Y.B. Band, P.S. Julienne, Phys. Rev. A 51 (1995) 4317.
[12] D. Leonhardt, J. Weiner, Phys. Rev. A 52 (1995) 4332.
[13] K.A. Suominen, J. Phys. B: At. Mol. Opt. Phys. 29 (1996) 5981.
[14] J.L. Bohn, P.S. Julienne, Phys. Rev. A 54 (1996) 4637.
[15] H. Wang, X.T. Wang, P.L. Gould, W.C. Stwalley, J. Chem. Phys. 106 (1997) 7899.
[16] H. Wang, W.C. Stwalley, J. Chem. Phys. 108 (1998) 5767.
[17] J. Qin, T.O. Nelson, D.W. Setser, J. Phys. Chem. 95 (1991) 5374.
[18] J.H. Schloss, R.B. Jones, J.G. Eden, J. Chem. Phys. 99 (1993) 6483.
[19] G. Lo, D.W. Setser, J. Chem. Phys. 100 (1994) 5432.
[20] A.W. McCown, J.G. Eden, J. Chem. Phys. 81 (1984) 2933.
[21] E.B. Gordon, V.G. Egorov, S.E. Nalivaiko, V.S. Pavlenko, O.S. Rzhevsky, Chem. Phys. Lett. 242 (1995) 75.
[22] G. Rodriguez, J.G. Eden, J. Chem. Phys. 95 (1991) 5539.
[23] J. Koperski, J.B. Atkinson, L. Krause, Chem. Phys. Lett. 219 (1994) 161.
[24] J. Koperski, J.B. Atkinson, L. Krause, Can. J. Phys. 72 (1994) 1070.
[25] P. Bicchi, C. Marinelli, R.A. Bernheim, Phys. Rev. A 56 (1997) 2025.
[26] U. Marvet, M. Dantus, Chem. Phys. Lett. 245 (1995) 393.
[27] H.M.J.M. Boesten, C.C. Tsai, B.J. Verhaar, D.J. Heinzen, Phys. Rev. Lett. 77 (1996) 5194.
[28] M. Machholm, A. Giusti-Suzor, F.H. Mies, Phys. Rev. A 50 (1994) 5025.
[29] I.D. Petsalakis, T. Mercouris, C.A. Nicolaides, Chem. Phys. 189 (1994) 615.
[30] P. Backhaus, B. Schmidt, Chem. Phys. 217 (1997) 131.
[31] P. Gross, M. Dantus, J. Chem. Phys 106 (1997) 8013.
[32] A. Vardi, D. Abrashkevich, E. Frishman, M. Shapiro, J. Chem. Phys. 107 (1997) 6166.
[33] H. Dietz, A. Materny, V. Engel, Chem. Phys. 217 (1997) 249.
[34] M.V. Korolkov, J. Manz, G.K. Paramonov, B. Schmidt, Chem. Phys. Lett. 260 (1996) 604.
[35] M.V. Korolkov, B. Schmidt, Chem. Phys. Lett. 272 (1997) 96.
[36] M.V. Korolkov, J. Manz, G.K. Paramonov, Chem. Phys. 217 (1997) 341.
[37] P. Backhaus, J. Manz, B. Schmidt, J. Phys. Chem. A 102 (1998) 4118.
[38] M.V. Korolkov, G.K. Paramonov, Phys. Rev. A. 57 (1998) 4998.
[39] J.N. Murrel, K.S. Sorbie, J. Chem. Soc. Faraday Trans. II 68 (1972) 1552.
[40] C.W. Bauschlicher, S.R. Langhoff, J. Chem. Phys. 87 (1987) 4665.
[41] W.J. Stevens, G. Das, A.C. Wahl, J. Chem. Phys. 61 (1974) 3686.
[42] S. Chu, M. Yoshimine, B. Liu, J. Chem. Phys. 61 (1974) 5389.
[43] S.R. Langhoff, E.F. van Dishoeck, R. Wetmore, A. Dalgarno, J. Chem. Phys. 77 (1982) 1379.
[44] R. Loudon, The Quantum Theory of Light, Clarendon, Oxford, 1973.
[45] R. Kosloff, Annu. Rev. Phys. Chem. 45 (1994) 145.
[46] M.D. Feit, J.A. Fleck Jr., A. Steiger, J. Comput. Phys. 47 (1982) 412.
[47] C.C. Marston, G.G. Balint-Kurti, J. Chem. Phys. 91 (1989) 3571.
[48] M.V. Korolkov, G.K. Paramonov, B. Schmidt, J. Chem. Phys. 105 (1996) 1862.
[49] J. Tellinghuisen, Adv. Chem. Phys. 60 (1985) 399.
[50] G. Scoles (Ed.), Atomic and Molecular Beam Methods, Oxford University, New York, 1988.
[51] G.K. Paramonov, in: J. Manz, L. Wöste (Eds.), Femtosecond Chemistry, Verlag Chemie, Weinheim, 1995, pp. 671–712.
[52] A.D. Bandrauk, S.C. Wallace (Eds.), Coherence Phenomena in Atoms and Molecules in Laser Fields, Plenum, New York, 1992.
[53] A. Giusti-Suzor, F.H. Mies, L.F. DiMauro, E. Charron, B. Yang, J. Phys. B. 28 (1995) 309.
[54] R. de Vivie, C.M. Marian, S.D. Peyerimhoff, Mol. Phys. 63 (1988) 3.
[55] I.V. Andrianov, G.K. Paramonov, Phys. Rev. Lett., submitted.
[56] D.R. Yarkony, J. Chem. Phys. 97 (1992) 1838.